

Three-dimensional Microstructure of Frozen Meniscus and Hook in Continuous-cast Ultra-low-carbon Steel Slabs

Go Gi, Lee

Pohang University of Science and Technology
San31, Hyoja-dong, Nam-gu, Pohang, Kyungbuk 790-784
South Korea
Tel: +82-54-279-2815
Fax: +82-54-279-2399
E-mail: yikoki@postech.ac.kr

Ho Jung, Shin

POSCO Technical Research Laboratories
699, Gumho-dong, Gwangyang, Jeonnam 545-090
South Korea
Tel: +82-61-790-8770
Fax: +82-61-790-9287
E-mail: ceraby@posco.co.kr

Brian G. Thomas

University of Illinois at Urbana-Champaign
1206 West Green Street
Urbana, IL 61801
Tel.: 217-333-6919
Fax: 217-244-6534
E-mail: bgthomas@uiuc.edu

Seon Hyo, Kim

Pohang University of Science and Technology
San31, Hyoja-dong, Nam-gu, Pohang, Kyungbuk 790-784
South Korea
Tel: +82-54-279-4315
Fax: +82-54-279-2399
E-mail: seonhyo@postech.ac.kr

Dong Su, Kim

POSCO Steelmaking Department
700, Gumho-dong, Gwangyang, Jeonnam 545-711
South Korea
Tel: +82-61-790-2210
E-mail: dongsookim@posco.co.kr

Sung Jong, Yu

POSCO Steelmaking Department
700, Gumho-dong, Gwangyang, Jeonnam 545-711
South Korea
Tel: +82-61-790-7410
E-mail: sjyu@posco.co.kr

Key words: Frozen meniscus shape, Conventional cast slab, Solidification structure, Surface quality, Hook

INTRODUCTION

Deep oscillation marks (OMs)^[1] and subsurface hooks^[2] in continuously-cast steel slabs are associated with many slab quality problems. Specifically, they tend to entrap argon bubbles and alumina inclusions near the hooks^[3, 4], leading to slivers and blisters, and transverse cracks often form near the roots of deep OMs^[5-7]. In extreme cases, the entire slab surface must be ground or “scarfed” to remove all traces of the hook microstructure, resulting in high cost and loss of productivity^[8]. As shown in Figure 1(a), subsurface hooks are distinctive micro-structural features which extend from some oscillation marks and can be identified by etching transverse sections near the slab surface^[1, 2, 6].

Hooks and OMs form due to many interdependent, transient phenomena that occur simultaneously during initial solidification near the meniscus. Several different mechanisms for hooks and OMs have been proposed in previously published literature. J. Sengupta et al.^[9, 10] have recently suggested a new mechanism for hooks and OMs formation with matching experimental observations, which is illustrated in Figure 1(b) ~ (e)^[9, 10]. Hook formation starts when undercooled liquid steel at the meniscus freezes. Overflow on the solidified meniscus then occurs when the new liquid meniscus becomes unstable, which usually happens at the beginning of the negative strip period^[11] during mold oscillation, causing a rapid increase of mold heat flux. Dendrites solidify away from the meniscus, which persists in the final microstructure as a distinct “line of hook origin”. The extent that the overflowing liquid steel can penetrate into the flux channel determines the final shape of the upper side of the OM. This mechanism was based on a careful analysis of numerous specially etched samples from ultra-low-carbon steel slabs in controlled plant trials^[8, 12] at POSCO. Furthermore, it is combined with literature review, theoretical modeling results^[11] and supported by microstructural evidence obtained using^[9] optical microscopy, scanning electron microscopy (SEM), electron backscattering diffraction (EBSD), energy dispersive X-ray spectroscopy (EDXS), and electron probe micro-analysis (EPMA) techniques.

The initial brittle fracture of the curved hook with entrapped bubbles in Figure 1(a) is explained by hot tearing of the fragile semi-solid near hook tip during overflow^[11], as shown in Figure 1(d). The fractured hook tip usually melts or is transported away by the flowing liquid steel and then it will be truncated hook, as shown in Figure 1(e), but a few micrographs contained a fractured hook tip that was captured nearby, proving this mechanism^[9, 11]. The slight microsegregation accompanying dendritic solidification showed that growth proceeded in both directions from the line of hook origin and the line of hook origin was found to divide regions of different orientation in the steel, even after several phase transformations^[9].

Previous understanding of hook and OM formation is based entirely on two-dimensional (2-D) vertical-section micrographs, such as Figure 1(a), which reasonably represent the microstructure around most of the slab perimeter. Near the corners of the slab, however, OMs and hooks exhibit complex 3-D shapes, with different internal microstructures that were unknown before this work.

The present study was conducted to reveal the complex 3-D shape of the frozen meniscus hooks and OMs near the slab corners in ultra-low-carbon steel samples. A variety of cross sections near the slab corners were specially etched and analyzed to distinguish the frozen meniscus shape, including vertical, horizontal, and angle sections at different depths and locations in three slab samples taken from the slab corners. The results provide unique evidence of sub-surface micro-structural evolution in the meniscus region near the slab corners of continuous-cast steel.

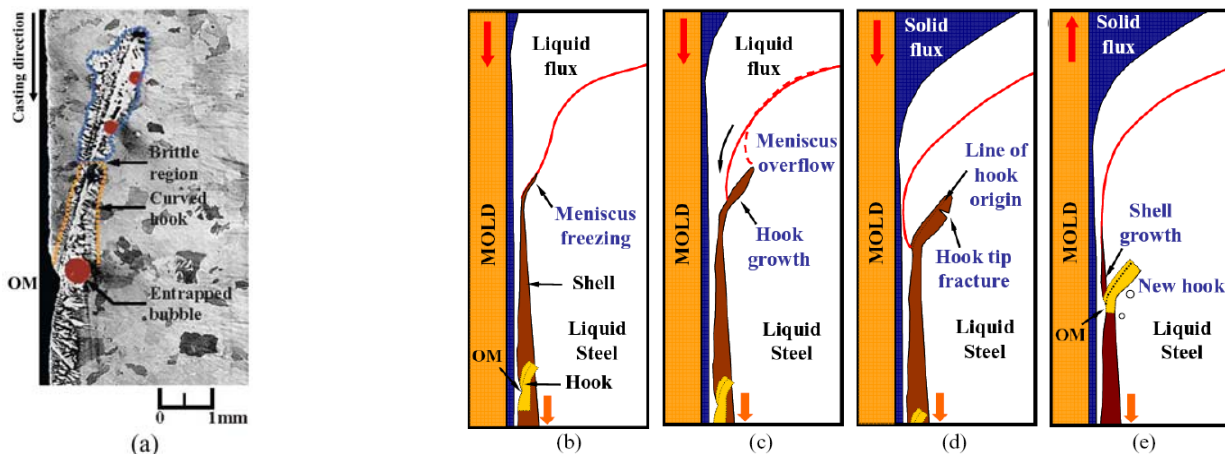


Figure 1 Optical micrograph of an ultralow-carbon steel sample showing (a) entrapment of argon bubble by a curved hook-type oscillation mark and (b)~(e)^[9, 10] schematic illustrating formation of curved hooks in an ultra-low-carbon steel slabs by meniscus solidification and subsequent liquid steel overflow

EXPERIMENTS

Samples from the slab corners of 230 X 1300mm ultra-low-carbon steel slabs were obtained from plant experiments performed on #2-1 conventional slab caster at POSCO, Gwangyang Works, South Korea, which features a conventional parallel-mold, standard two-port submerged entry nozzle, non-sinusoidal hydraulic mold oscillator and electromagnetic brake ruler system. The casting speed was kept relatively constant at 1.45m/min. Table 1 summarizes the casting conditions employed during casting of the slabs that contained the samples. The casting conditions of samples I, II, and III match the conditions of Tests 3, 9 and 10 in reference^[12] respectively. Further details of these plant experiments, including the composition of the ultra-low-carbon steel grade and mold powder is given elsewhere^[12].

Table 1 Casting conditions for slab samples

Sample number	Pour temperature (°C)	Mold oscillation stroke (mm)	Mold oscillation frequency (cpm)	Non-sinusoidal mold oscillation ration (%)
Sample I	1571	5	174	12
Sample II	1559	7	145	0
Sample III	1559	7	125	12

Sample I (13mm wide x 20mm deep x 100mm long and encompassing 10 OMs) was obtained near the corner and was divided into three pieces each about 30mm long, as shown in Figure 2(a). Each sample was taken vertical sections at various distances (0.5 to ~5.5mm) from the wide face surface, by polishing, etching, photographing, and then regrinding at intervals of about 0.5mm, as shown in Figure 2(b). These sections parallel to the wide face revealed characteristic subsurface microstructural features, which were interpreted by extracting hook shapes to construct the 3-D hook shape. Further vertical sections were taken at 20mm, 75mm and 115mm (center line) of sample I-2 from the slab corner from the same slab and hook depths and shapes were measured from micrographs of each section.

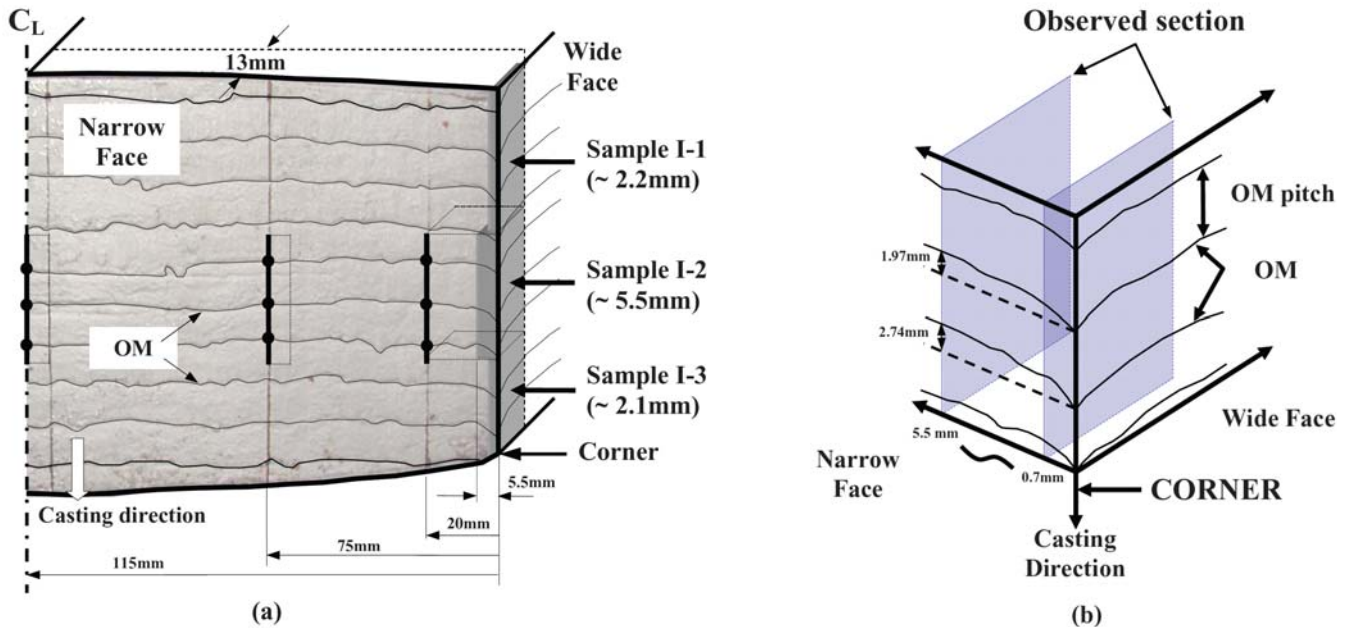


Figure 2 Sample I (a) location obtained from slab corners and (b) location of sections cut for microscopy analysis showing oscillation mark shape

Sample II (100mm long and encompassing 9 OMs) was obtained near the corner from a different slab and was divided into three pieces each about 30mm long, as shown in Figure 3(a). Each sample was then cut at a different vertical orientation to reveal the subsurface microstructures, as shown in Figure 3(b) through (d).

Sample III (20mm long and encompassing 2 OMs) was obtained near the corner from a third slab and was cut horizontally through the tip of the oscillation marks at the corner, as shown Figure 4(a). Optical micrographs of the samples were obtained at 0.3mm, 0.8mm, and 1.0mm cross section surfaces from cutting section shown in Figure 4(b), and are presented in Figure 5 for the 1st oscillation mark.

Further slab samples were taken for other conditions (Heats 4~5^[8]) and hook depths were measured from vertical sections taken from each sample around the perimeter of the narrow face (5 locations) and wide face (7 locations).

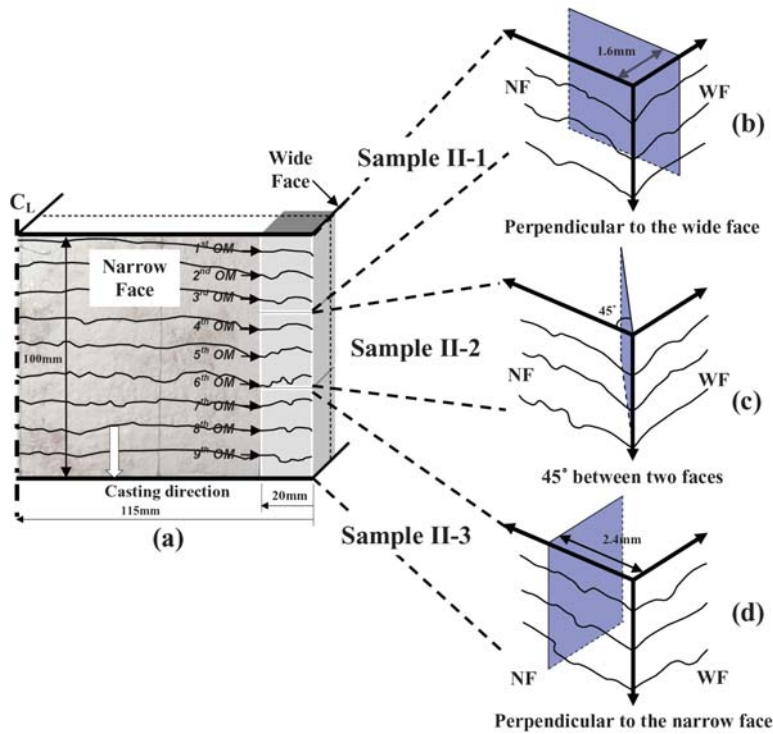


Figure 3 Sample II (a) location obtained from slab corners and (b)~(d) orientation of three different vertical sections cut for microscopy analysis

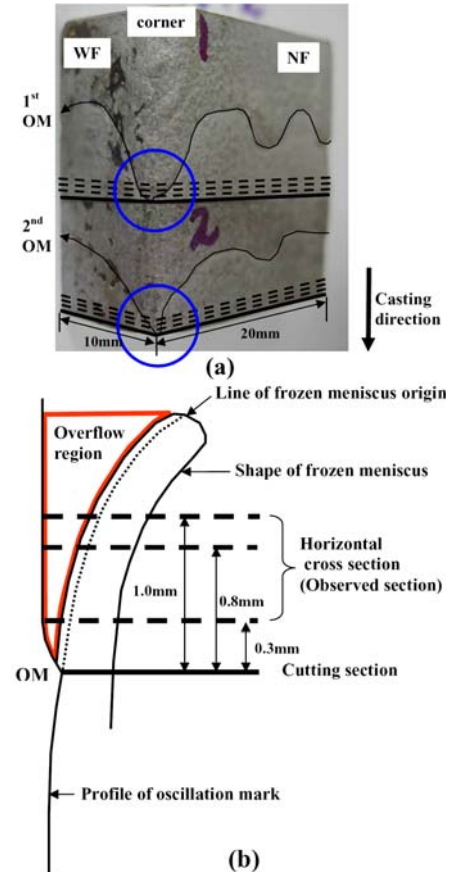


Figure 4 Sample III (a) location obtained from slab corner and (b) three different horizontal sections cut for microscopy analysis of hooks and oscillation mark shown in circles

All of the sections were ground, polished, and then etched by a special etching method^[9] to reveal the microstructure and hook shapes in ultra-low-carbon steel samples. The etching reagent was picric acid solution (2, 4, 6-trinitrophenol) with additions of surfactant zephiramine (benzyltrimethyl-n-tetradecylammonium chloride) and etched for ~1-1.5 h. Further details are given elsewhere^[9].

RESULTS AND DISCUSSIONS

Overflow Mechanism of Liquid Steel at the Corner

Oscillation marks are well known to “point” downwards at the corners, indicating the casting direction, as in Figure 4(a). The lowest point of each oscillation mark is found at the corner, extending 2-3mm below the average around the perimeter, as shown in Figure 2 (b). The reason for this is clarified by analysis of the horizontal section micrographs in Figures 4 and 5, which also reveal new insights into hook and OM formation in the slab corner.

Each micrograph in Figure 5 exhibits two distinct layers of frozen steel at the corner, which formed at different times. The schematic in Figure 4(b), explains the appearance of these microstructural features. A long, thin layer bounded by a faint dark band runs around the corner subsurface. This band is a slice through the base of the hook, which was originally the frozen meniscus. A small layer found on the surface at the corner, (outlined) decreases in size with decreasing vertical distance to the OM point (i.e. from 1.3 to 0.8 to 0.3mm). The enlarged inset in Figure 5(c) clearly shows OM valleys on each side of this surface layer, indicating that it formed later, from liquid running down the surface.

After the 3-D meniscus in the corner freezes to form the hook, liquid steel overflows into the corner gap between the frozen meniscus and the mold. As the overflowing liquid freezes, its cross section naturally becomes smaller with decreasing distance towards the OM point. The tip of this overflowed region penetrates further into the corner, where the gap between the mold and the frozen meniscus hook is largest. This larger gap also explains why the hook is thinner in the corner, as it decreases heat transfer.

Variation of Frozen Meniscus Shape near Corner

Micrographs of hooks near the slab corner show a wide variation of size and shape, as shown in a series of 11 hooks in Figure 6 taken ~2mm from wide face surface for 4.1sec of casting. This wide variation indicates that the shape of the meniscus depends on complex events dictated by time-dependent local phenomena near the meniscus, such as variations in superheat delivery due to fluid flow.

The curved line along the center of each hook represents the “line of origin” of the frozen meniscus, and indicates the shape of the initial meniscus when it froze. Note the discontinuous hook on the far left, provides further evidence of meniscus freezing, as it indicates a portion of the meniscus either did not freeze, or later melted.

Analysis of 3-D Subsurface Frozen Meniscus and Hook Shape around the Corner

Micrographs of vertical sections presented in Figure 7 show great differences in frozen meniscus and hook shape near the corner. Solidification proceeded in both directions away from line of frozen meniscus origin, slowing temporarily when thermal gradients diminished, to leave the dark bands that outline each frozen meniscus. The lines of frozen meniscus origin traced from a series of ten such vertical sections with profile of OM's are shown in Figure 8(a). A true three-dimensional schematic of the frozen meniscus and hook shape around slab corner, given in Figure 8(b), was constructed from the meniscus outlines surrounding the 2nd OM. The upper lines (blue-solid) outline the liquid that overflowed the frozen meniscus. The lower lines (red-dashed) indicate the boundary between the supercooled frozen meniscus and the molten steel pool below.

Figure 9(a) was constructed to show the top view of the three OM hooks in Figure 8(a). This graph clearly reveals the three-dimensional shape of the frozen meniscus and hooks, which extends continuously from the OM perimeter around the slab corner. The schematic in Figure 9(b) was constructed to explain the different hook microstructures observed near the slab corner. The 3rd OM hook is consistently smaller than its neighbors, for example. This indicates that changes in meniscus conditions extending around the corner but lasting less than a second are very common. This is likely due to transient fluid-flow phenomena, such as surface level and superheat fluctuations, which vary even under steady casting conditions. Figure 9(b) explains the observation in Figure 7 that the 2nd OM hook is triple the depth of the 3rd OM at 2.5 mm from the corner, but only twice the depth at 3.5mm.

Concave Curvature of Frozen Meniscus at Corner

The micrograph in Figure 10(a) shows the deepest extent of the hooks, which is observed in a 45 degree vertical cross section from the corner, as shown in Figure 3(c). Figure 10(b) shows the approximate 3-D hook shape constructed from different vertical sections through different oscillation marks near the corner. The hooks at the corner start about 0.75mm lower than other two nearby observations. This indicates the downward pointing OM caused by the furthest penetration of overflowing liquid steel into the flux channel at the corners, as discussed earlier.

Figure 10(b) also shows that corner hooks exhibit a concave curvature. At other locations, including previous work^[8, 9, 11-13], this was not observed. This concave curvature, furthermore, is not predicted for the two-dimensional equilibrium meniscus shape by Bikerman's equation^[14, 15]. This observation suggests that other effects, such as transient pressure variations caused by the moving slag rim attached to the mold wall are more influential near the slab corners than elsewhere. This is consistent with a thicker solidified flux rim in the colder corners.

Hook Shape around Slab Perimeter

Figure 11 compares hook depths around the perimeter of slab sample I-2, as shown in Figure 2(a). The maximum hook depth appears at the corners, owing to further meniscus solidification, likely due to the colder liquid found in this region. Differences between inner and outer radius are negligible. Hook depths^[8] measured around the slab perimeter are shown Figure 12. Hooks extend continuously around the entire slab perimeter, although they are often difficult to etch. The hooks are always deepest at the corners, by 10 to 100%. Hooks are often deeper towards the narrow faces although significant asymmetry is observed between sides.

Comparison of Frozen Meniscus Shape with Measurements and Previous Predictions

Figure 13(a) shows lines of the frozen meniscus origin at different distances from the wide face surface near the slab corners obtained from 2nd OM in Sample I-2, compared with Bikerman's equation^[14, 15]. The actual hook shape measured from the micrographs is compared in Figure 13(b) with previous mathematical model predictions, including 1) Bikerman's equation; 2) thermal distortion of a solidified shell after a surface level fluctuation^[9, 11], and 3) the meniscus shape caused by alternating pressure in the liquid slag and steel due to oscillation of the mold and attached slag rim^[13].

Far from the corner, Figure 13 (b), the measurements match well with the equilibrium shape from Bikerman's equation and the transient model predictions^[13]. Measurements near the corners, Figure 13 (a), exhibit a frozen meniscus shape which is more curved (lower) than the shape from the 2-D Bikerman's equation. This is likely because 3-D surface tension effects cause more curvature near the corner. In addition, the larger slag rim in the corner leads to higher transient pressure during the oscillation downstroke, causing more depression of the meniscus. The extra curvature allows the overflowing steel to penetrate deeper down the corners. Corner hooks are also longer (deeper) than elsewhere, likely due to the generally lower superheat found near the corners.

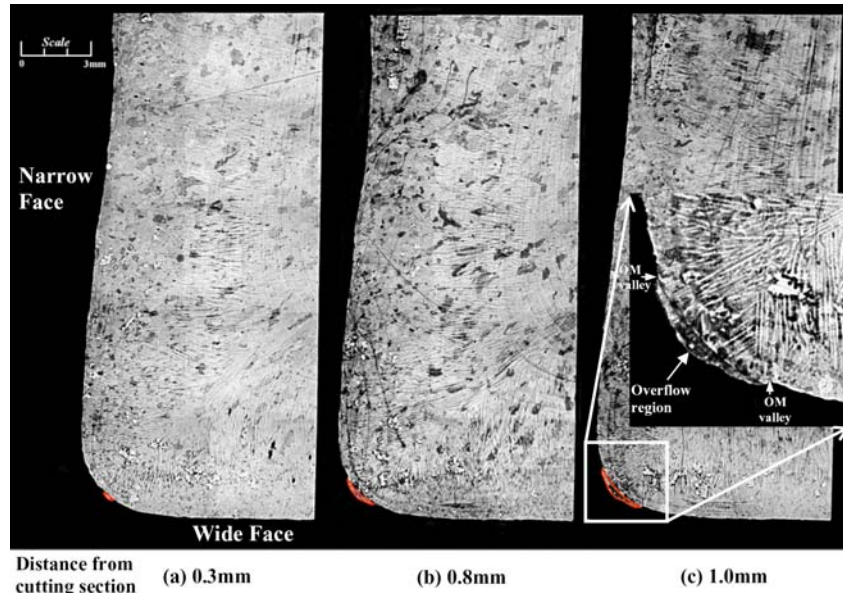


Figure 5 Optical micrographs of horizontal cross sections (Sample III) showing evidence of liquid steel overflow

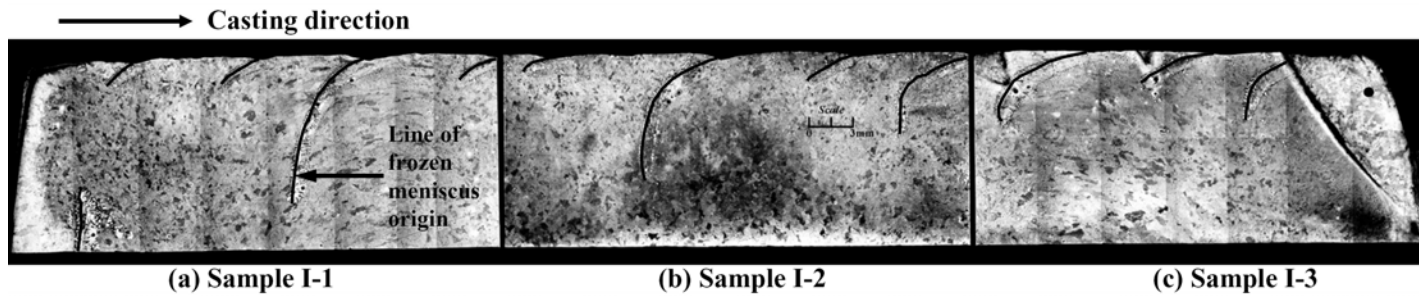


Figure 6 Optical micrographs at (a), (b) 2.2mm and (c) 2.1mm distance from wide face (sample I-1~I-3) showing variation of meniscus shape near the corners

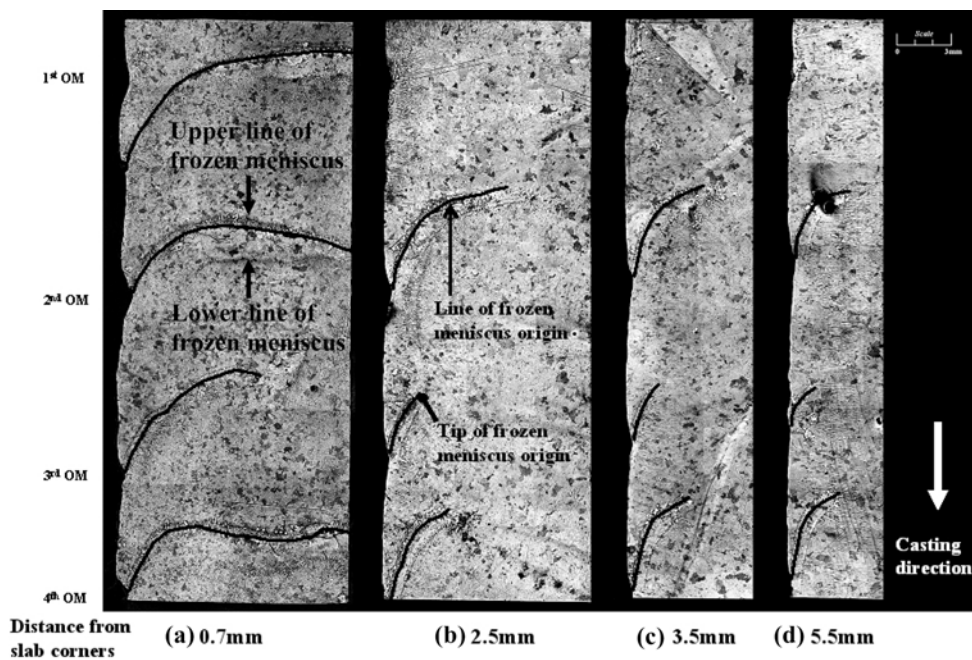


Figure 7 Optical micrographs at different distances from wide face (sample I-2) showing line of frozen meniscus origin: "hooks"

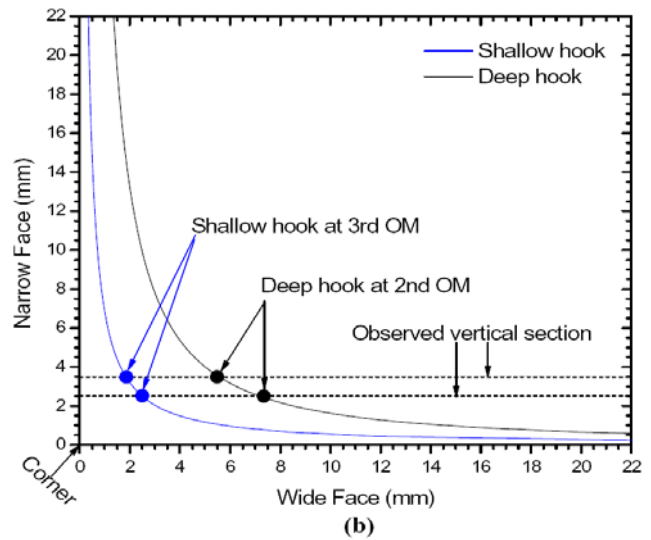
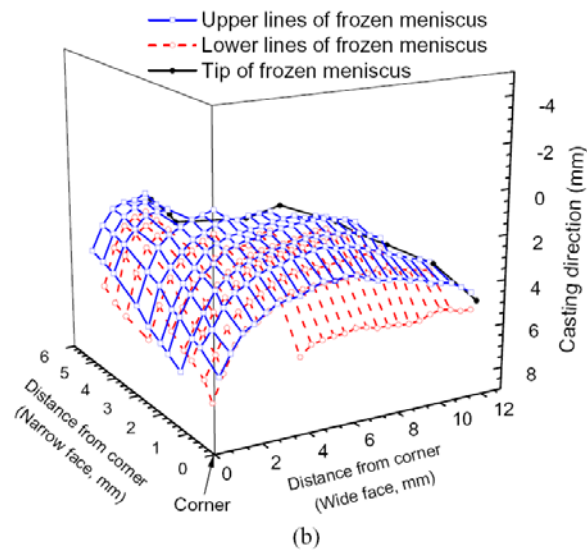
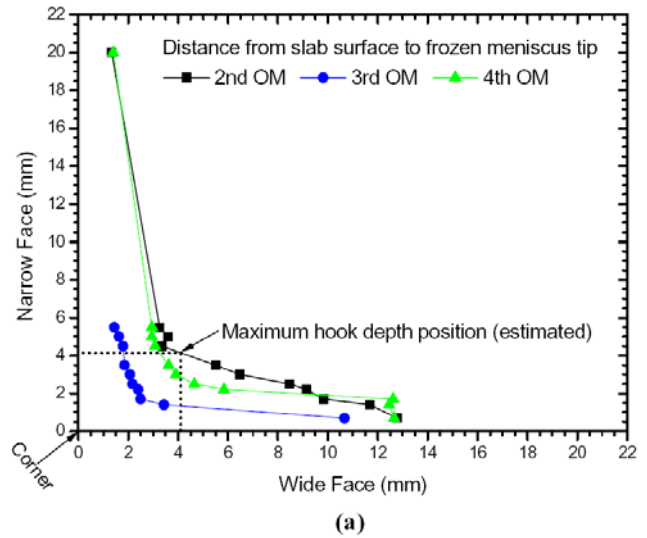
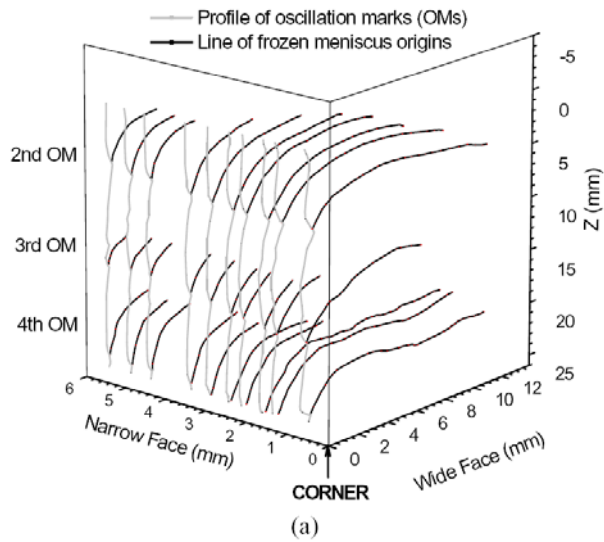


Figure 8 Line of frozen meniscus origins obtained from micrograph analysis of Sample I-2 (a) and (b) 3-D shape of frozen meniscus hook at 2nd OM

Figure 9 Top views of lines of frozen meniscus origins (hooks) from micrographs (Sample I) showing (a) hook depth increase around slab corner and (b) explanation of hook depth variations observed in micrographs

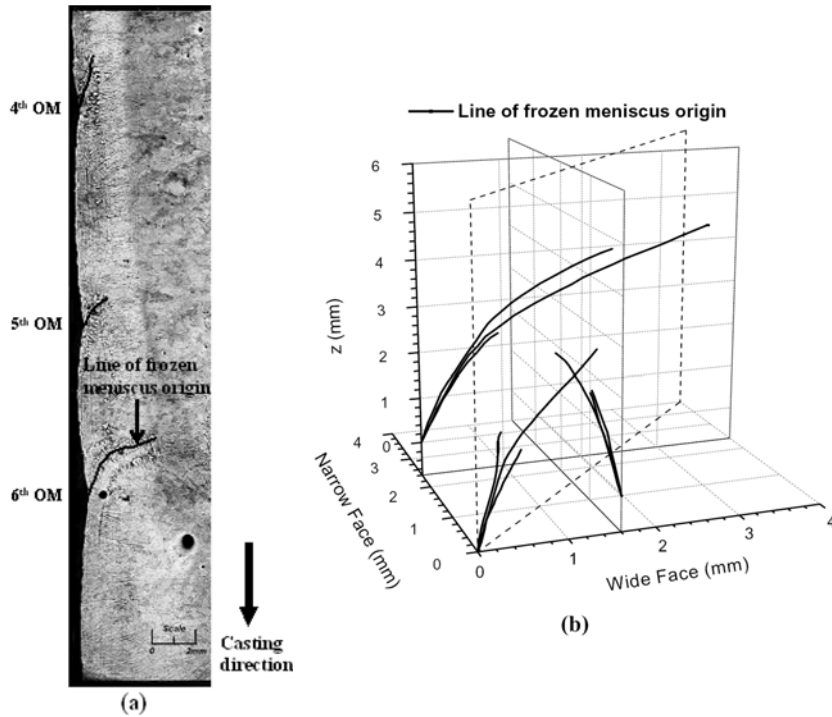


Figure 10 Hook shapes (lines of frozen meniscus from vertical sections through sample II) (a) micrograph of 45 degree section and (b) shapes traced from three different hooks

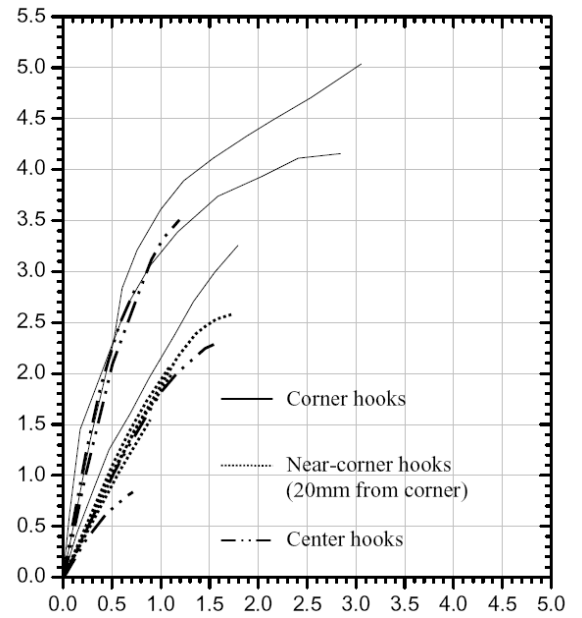


Figure 11 Lines of frozen meniscus (sample I-2) at three locations around slab perimeter of narrow face, showing increase in hook size towards corner

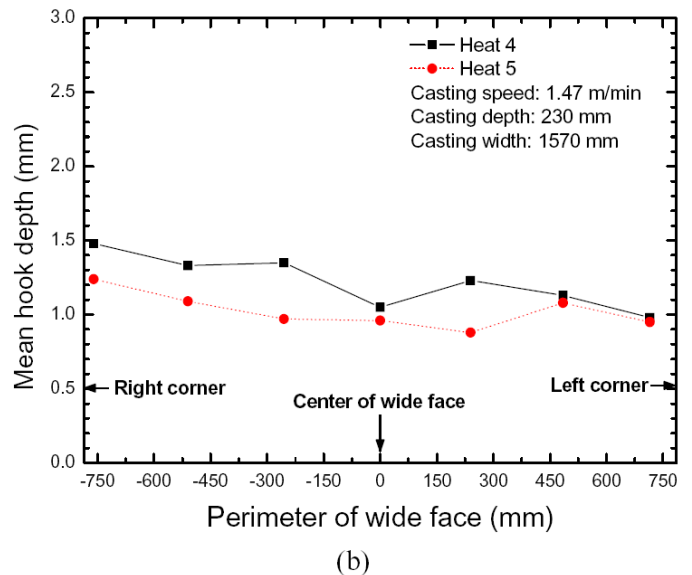
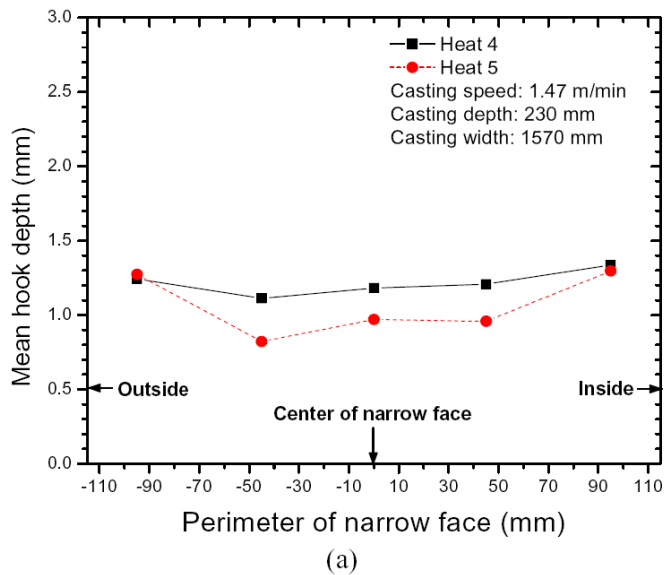


Figure 12 Hook depth variation along mold perimeter of (a) narrow face and (b) wide face

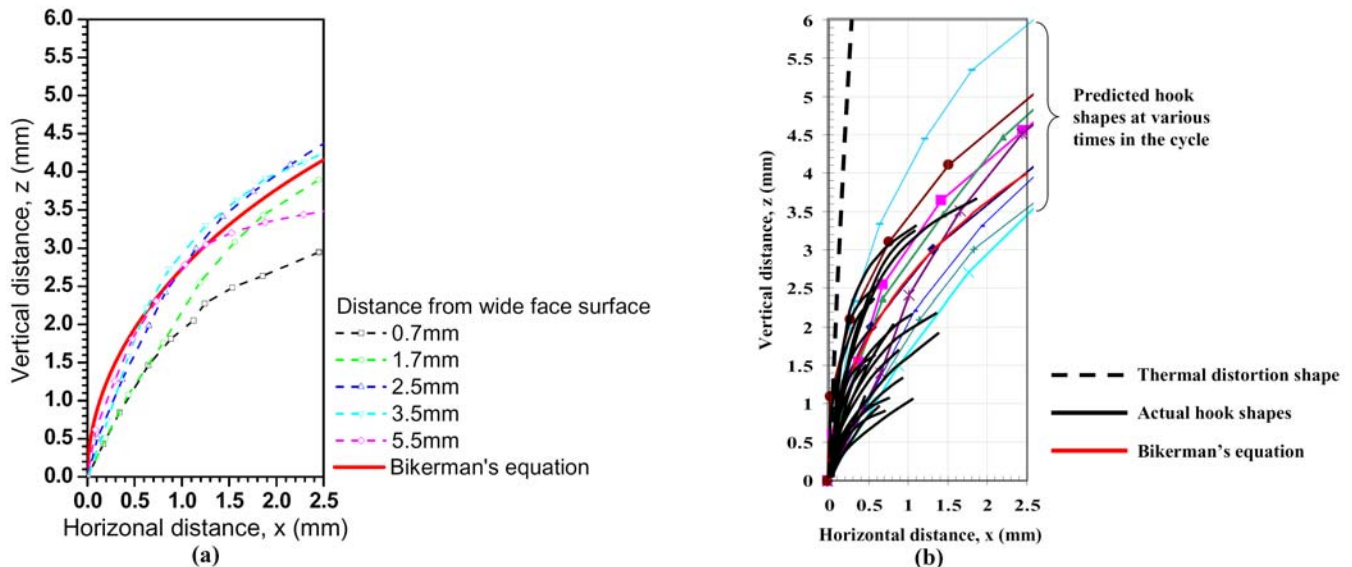


Figure 13 Comparison of meniscus shape: (a) measurements near the slab corners and (b) comparison between the actual and predicted^[13] hook shapes far from slab corners

CONCLUSIONS

The 3-D shape of the frozen meniscus, subsurface hook microstructure, and oscillation marks in continuous-cast ultra-low carbon steel slabs has been investigated by analyzing micrographs of carefully-etched samples near the corners. The specific results of this study provide the insight the shape of frozen meniscus and the mechanism of hook and oscillation mark formation:

1. Oscillation marks extend further in the casting direction at the corner due to the ease of liquid steel overflow into the larger gap there. The horizontal sections provide clear evidence that OM's formation due to liquid steel overflow. The line of hook origin in the subsurface microstructure indicates the original shape of the frozen meniscus.
2. Concave curvature on 45 degree vertical cross section and variation of frozen meniscus shape compared with previous studies including modeling results, other effects such as lower superheat and higher pressure due to thicker flux rim during mold oscillation greatly affects the meniscus shape near the corners. Deeper hooks in this region may be affected by these effects.
3. A graphical reconstruction of the 3-D hook shape in the corner from a series of vertical cross sections explains the progression of 2-D hook microstructures observed around the slab perimeter.
4. The classic 2-D hook microstructure simply curves continuously around the corner, increasing in size towards the corner. Observation of maximum hook at the corner matches the expected shape of hook origin from 2-D hook measurement with mold perimeter. This shows the continuity of hook and oscillation mark formation around mold perimeter.
5. These results will provide a foundation for future computational models and plant trials to understand and control hook and OM formation near the slab corners.

ACKNOWLEDGEMENTS

The authors are grateful to Korea Research Foundation, South Korea (Grant KRF-2005-213-D00110) for financial support, and to the Continuous Casting Consortium at the University of Illinois at Urbana-Champaign for support of this project.

REFERENCES

1. Takeuchi, E. and J.K. Brimacombe, *The Formation of Oscillation Marks in the Continuous Casting of Steel Slabs*. Metallurgical Transactions, 1984. **15B**(Sept.): p. 493-509.
2. Emi, T., et al. *Influence of Physical and Chemical Properties of Mold Powders on the Solidification and Occurrence of Surface Defects of Strand Cast Slabs*. in *Steelmaking Conference Proceedings*. 1978: ISS-AIME.
3. K.-D.Schmidt, et al., *Consequent Improvement of Surface Quality by Systematic Analysis of Slabs*. Steel Research International, 2003. **74**(11/12.): p. 659-66.
4. Birat, J.-P., et al. *The Continuous Casting Mold: A Basic Tool for Surface Quality and Strand Productivity*. in *Steelmaking Conference Proceedings*. 1991: ISS.
5. Brimacombe, J.K. and K. Sorimachi, *Crack Formation in the Continuous Casting of Steel*. Metallurgical Transactions, 1977. **8B**: p. 489-505.
6. Takeuchi, E. and J.K. Brimacombe, *Effect of Oscillation-Mark Formation on the Surface Quality of Continuously cast Steel Slabs*. Metallurgical Transactions, 1985. **16B**(Sept.): p. 605-625.

7. Harada, S., et al., *A Formation Mechanism of Transverse Cracks on Continuously Cast Slab Surface*. ISIJ International, 1990. **30**(4): p. 310-316.
8. Shin, H.-J., et al. *Analysis of Hook Formation Mechanism in Ultra Low Carbon Steel using CONID Heat Flow Solidification Model*. in *MS&T 2004*. 2004. New Orleans, LA: The Association for Iron and Steel Technology (AISTech) and TMS.
9. Sengupta, J., et al., *Micrograph evidence of meniscus solidification and sub-surface microstructure evolution in continuous-cast ultralow-carbon steels*. Acta Materialia, 2006. **54**(No. 4): p. 1165-1173.
10. Sengupta, J., et al. *Mechanism of Hook Formation in Ultra-low Carbon Steel based on Microscopy Analysis and Thermal-stress Modeling*. in *AISTech 2006*. 2006. Cleveland, OH: The Association for Iron & Steel Technology (AISTech).
11. Sengupta, J., et al., *A New Mechanism of Hook Formation during Continuous Casting of Ultra-low-carbon Steel Slabs*. Metallurgical and Materials Transactions A, 2006. **37A**(No. 5): p. 1597-1611.
12. Shin, H.-J., et al. *Effect of Mold Oscillation on Powder Consumption and Hook Formation in Ultra Low Carbon Steel Slabs*. in *AISTech 2004*. 2004. Nashville, TN: The Association for Iron & Steel Technology.
13. Ojeda, C., et al. *Mathematical Modeling of Thermal-Fluid Flow in the Meniscus Region During An Oscillation Cycle*. in *AISTech 2006*. 2006. Cleveland, OH: The Association for Iron & Steel Technology (AISTech).
14. Bikerman, J.J., *Physical surfaces*. 1970, New York (NY): Academic Press.
15. Fredriksson, H. and J. Elfsberg, *Thoughts about the Initial Solidification Process during Continuous Casting of Steel*. Scandinavian Journal of Metallurgy, 2002. **31**(No. 5): p. 292-297.